Video Article

Fabrication and Operation of a Nano-Optical Conveyor Belt

Jason Ryan[1], Yuxin Zheng[1], Paul Hansen[1], Lambertus Hesselink[2]

[1]Electrical Engineering, Stanford University

[2]Applied Physics, Stanford University

Correspondence to: Jason Ryan at jdrjason@gmail.com

URL: http://www.jove.com/video/52842
DOI: doi:10.3791/52842

Keywords: Engineering, Issue 102, Plasmonics, optical trapping, near-field trapping, nano-optical conveyor belt, C-shaped aperture, optical tweezers, lab-on-a-chip, nanotechnology, C-shaped engraving, CSE, electron beam lithography, nanostructure

Date Published: 8/26/2015

Citation: Ryan, J., Zheng, Y., Hansen, P., Hesselink, L. Fabrication and Operation of a Nano-Optical Conveyor Belt. *J. Vis. Exp.* (102), e52842, doi:10.3791/52842 (2015).

Abstract

The technique of using focused laser beams to trap and exert forces on small particles has enabled many pivotal discoveries in the nanoscale biological and physical sciences over the past few decades. The progress made in this field invites further study of even smaller systems and at a larger scale, with tools that could be distributed more easily and made more widely available. Unfortunately, the fundamental laws of diffraction limit the minimum size of the focal spot of a laser beam, which makes particles smaller than a half-wavelength in diameter hard to trap and generally prevents an operator from discriminating between particles which are closer together than one half-wavelength. This precludes the optical manipulation of many closely-spaced nanoparticles and limits the resolution of optical-mechanical systems. Furthermore, manipulation using focused beams requires beam-forming or steering optics, which can be very bulky and expensive. To address these limitations in the system scalability of conventional optical trapping our lab has devised an alternative technique which utilizes near-field optics to move particles across a chip. Instead of focusing laser beams in the far-field, the optical near field of plasmonic resonators produces the necessary local optical intensity enhancement to overcome the restrictions of diffraction and manipulate particles at higher resolution. Closely-spaced resonators produce strong optical traps which can be addressed to mediate the hand-off of particles from one to the next in a conveyor-belt-like fashion. Here, we describe how to design and produce a conveyor belt using a gold surface patterned with plasmonic C-shaped resonators and how to operate it with polarized laser light to achieve super-resolution nanoparticle manipulation and transport. The nano-optical conveyor belt chip can be produced using lithography techniques and easily packaged and distributed.

Video Link

The video component of this article can be found at http://www.jove.com/video/52842/

Introduction

Capture, interrogation and manipulation of single nanoparticles are of growing importance in nanotechnology. Optical tweezers have become a particularly successful manipulation technique for experiments in molecular biology[1-4], chemistry[5-7] and nano-assembly[7-10], where they have enabled breakthrough experiments such as the measurement of the mechanical properties of single DNA molecules[4] and the sorting of cells by their optical properties[11,12]. Discoveries on these frontiers open up the study of even smaller systems, and they make way for the engineering of new practically beneficial products and techniques. In turn, this trend drives the need for new techniques to manipulate smaller, more rudimentary particles. In addition, there is a push to build 'lab-on-a-chip' devices to perform these functions more cheaply and in a smaller package in order to bring chemical and biological tests out of the lab and into the field for medical and other purposes[13,14].

Unfortunately, conventional optical trapping (COT) cannot meet all of nanotechnology's growing demands. COT operates on the mechanism of using a high numerical aperture (N.A.) objective lens to bring laser light to a tight focus, creating a localized peak in optical intensity and high gradients in the electromagnetic field energy. These energy density gradients exert a net force on light-scattering particles which generally draws them in towards the center of the focus. Trapping smaller particles requires higher optical power or a tighter focus. However, focused beams of light obey the principle of diffraction, which limits the minimal size of the focal spot and places an upper bound on the energy density gradient. This has two immediate consequences: COT cannot trap small objects efficiently, and COT has trouble discriminating between closely spaced particles, a trapping resolution limitation known as the 'fat fingers' problem. In addition, implementing multiple particle trapping with COT requires systems of beam-steering optics or spatial light modulators, components which drastically increase the cost and complexity of an optical trapping system.

One way to circumvent the fundamental limitations of conventional focused beams of light, said to propagate in the far field, is to instead exploit the gradients of optical electromagnetic energy in the near field. The near field decays exponentially away from sources of electromagnetic fields, which means that not only is it highly localized to these sources, but it also exhibits very high gradients in its energy density. The near fields of nano-metallic resonators, such as bowtie apertures, nano pillars, and C-shaped engravings, have been shown to exhibit extraordinary concentrations of electromagnetic energy, further enhanced by the plasmonic action of gold and silver at near-infrared and optical wavelengths. These resonators have been used to trap extremely small particles at high efficiency and resolution[15-22]. While this technique has proven

Copyright © 2015 Journal of Visualized Experiments

effective at trapping small particles, it has also proven to be limited in its ability to transport particles over appreciable range, which is necessary if near-field systems are to interface with far-field systems or microfluidics.

Recently, our group has proposed a solution to this problem. When resonators are placed very close together, a particle can in principle migrate from one near-field optical trap to the next without being released from the surface. The direction of transport can be determined if adjacent traps can be turned on and off separately. A linear array of three or more addressable resonators, in which each resonator is sensitive to a polarization or wavelength of light different from that of its neighbors, works as an optical conveyor belt, transporting nanoparticles over a distance of several microns on a chip.

The so-called 'Nano-Optical Conveyor Belt' (NOCB) is unique among plasmonic resonator trapping schemes, as not only can it hold particles in place, but it can also move them at high speed along patterned tracks, gather or disperse particles, mix and queue them, and even sort them by properties such as their mobility[23]. All of these functions are controlled by modulating the polarization or wavelength of illumination, with no need for beam-steering optics. As a near-field optical trap, the NOCB trapping resolution is higher than that of conventional focused-beam optical traps, so it can differentiate between particles in close proximity; because it uses a metal nanostructure to concentrate light into a trapping well, it is power-efficient, and does not require expensive optical components such as a high N.A. objective. Furthermore, many NOCBs may be operated in parallel, at high packing density, on the same substrate, and 1 W of power can drive over 1200 apertures[23].

We have recently demonstrated the first polarization-driven NOCB, smoothly propelling a nanoparticle back and forth along a 4.5 μm track[24]. In this article we present the steps necessary to design and fabricate the device, optically activate it and reproduce the transport experiment. We hope that making this technique more widely available will help bridge the size gap between microfluidics, far-field optics, and nanoscale devices and experiments.

Protocol

1. Design the C-shaped Engraving (CSE) Array

1. Design the array pattern.

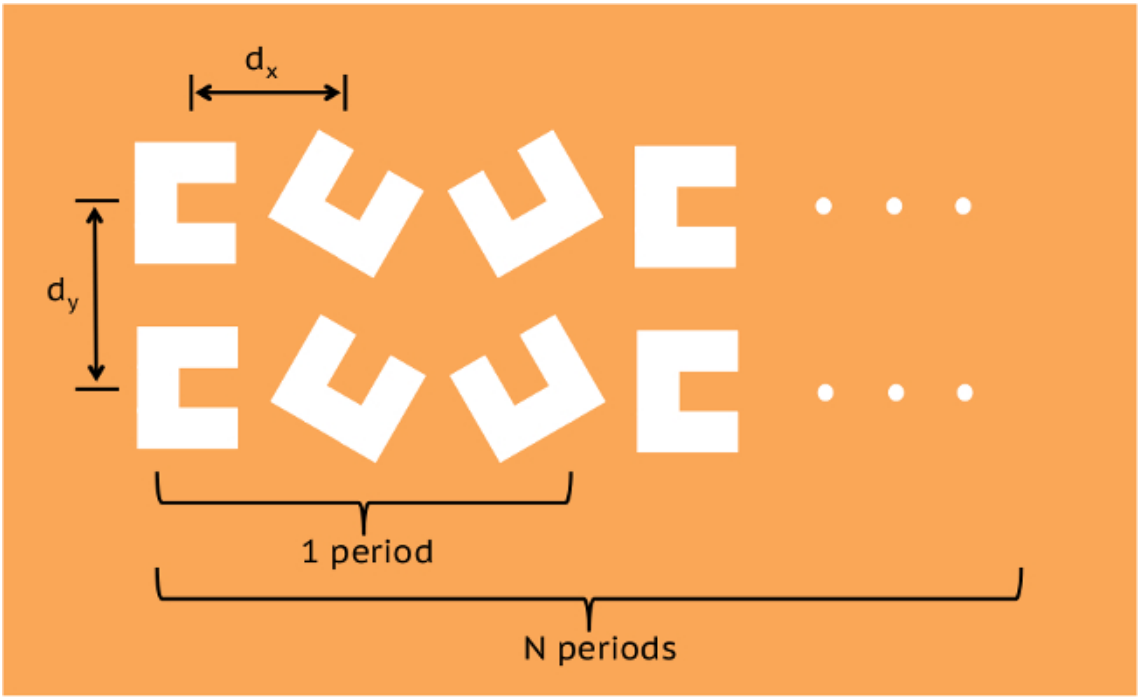

Figure 1. CSE Layout. Depiction of conveyor belt repeating element. Successful transport has been achieved using d_y = 320 nm and d_x = 360 nm. Adjacent pairs of engravings have a 60º relative rotational offset. Please click here to view a larger version of this figure.

1. Determine the desired path of particles across a planar substrate.
2. Using a CAD program, generate a double-linear array of C-shaped polygons along the path, each polygon in each pair consecutively rotated 30 ± 90° about its convex hull as shown in **Figure 1**. Because a particle's own volume roughly determines its handoff range[22], leave no more than one particle diameter separating consecutive pairs, and leave no more than 90% of this distance between polygon centers in a pair. Note: For reference, previous studies have indicated that polystyrene spheres of 390 nm in diameter and above are most suitable for transport along such a CSE array. Beads as small as 200 nm can be manipulated, though not reliably. However, beads larger than 500 nm feel stronger competing forces from a focused illumination beam.

2. Verify handoff forces along the array pattern using a numerical method to solve Maxwell's equations. While the procedure described herein pertains to the Finite Element Method (FEM) implemented by the commercial software COMSOL, it is possible to adapt this method for other numerical methods and implementations.

1. Draw up a numerical method geometry which accommodates the planar pattern dimensions and extends at least 200 nm below the pattern plane and 600 nm above the plane. Below the plane, include a domain to represent the substrate and above the plane a domain to represent the fluid chamber. Extrude the planar C-shaped pattern 150 nm downwards into the substrate, creating 3D domains to represent the interior of the engravings. Introduce a particle domain with the desired shape.
    1. Make sure that there is at least 200 nm of space between the top of the particle and the ceiling of the simulation volume and adjust the simulation extents as necessary. Add perfectly-matched layers at least 500 nm in thickness to the open boundaries of the simulation to absorb outward radiation.

2. Set the electromagnetic material properties of the domain above the interface to those of water, the material properties of the interior of the C-shaped engravings to those of hydrogen-silsesquioxane (HSQ), and the material properties of the remaining material to those of gold. Set the material properties of the particle to those of polystyrene or another material of choice. For simplicity, use linear electromagnetic material models.
   Note: A sample complete 3D geometry is shown in **Figure 2**. In this case, PML material domains at the Cartesian ±*x*, ±*y*, and +*z* boundaries absorb fields meant to propagate to infinity. PML thickness is defined to be 5 times the maximum tetrahedral mesh element size, equal to 5 x 100 nm = 500 nm.
3. If permittivity ε_r and permeability μ_r are required inputs for the numerical solver at hand, use a relative permittivity of 1.96 for HSQ, 1.77 for water, and -52.15 - 3.57i for gold. Set all relative permeabilities to 1. If an electromagnetic material property other than permittivity and permeability are required, use these values to derive the required inputs according to standard electromagnetic identities. Use the appropriate sign of the imaginary part of gold according to the complex time harmonic sign convention of the numerical solver (it should be negative under the exp(+*iωt*) convention and positive under the exp(-*iωt*) convention).

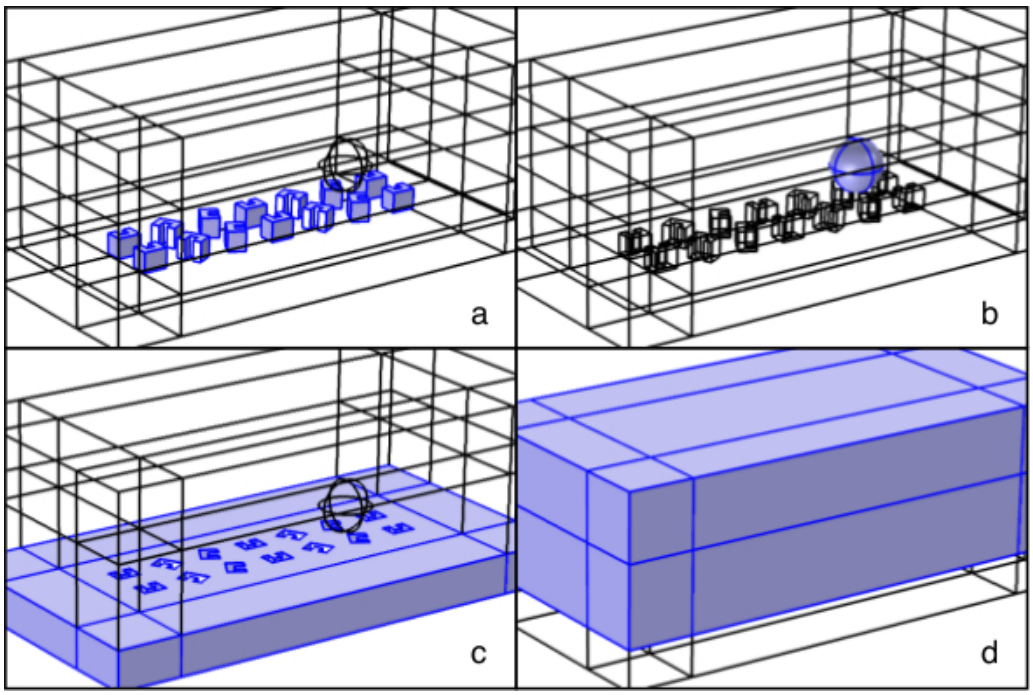

Figure 2. Simulation Geometry. Example of numerical simulation geometry in the commercial Finite Element Method software COMSOL. Two conveyor belt periods are simulated with d_y = 320 nm and d_x = 360 nm and a 500 nm diameter sphere. Shaded material regions are a) HSQ, b) polystyrene, c) gold, and d) water. Please click here to view a larger version of this figure.

4. Discretize the simulation volume with an adaptive tetrahedral mesh. Constrain the maximum size of the mesh elements to no larger than 100 nm in the bulk. Furthermore, constrain the maximum size of mesh elements to 30 nm on the sphere surface and 30 nm on the engraving surfaces to increase accuracy on critical structures. A moderate mesh growth rate of about 1.4 should be used to preserve mesh element quality in those regions, and a minimum mesh size can also be defined in the volume to limit unpredictable adaptive mesh behavior.
5. For optical excitation, define a background harmonic plane wave with a free space wavelength of 1,064 nm which is normally incident and reflected off of the planar gold substrate as if the engravings and particle were absent. Use the Fresnel equations evaluated at a normal angle of incidence to calculate plane wave reflection and transmission coefficients. Choose the polarization of this wave such that the electric field is aligned with the ridge of a C-shaped engraving. Normalize the intensity of the plane wave to 1 mW/μm^2.
6. Solve for the scattered electromagnetic fields in a batch of simulations, sweeping the particle position parameter from one end of the path to the other while holding the particle's altitude constant at just a few nanometers off the surface. Altitudes as low as 5 nm tend to predict very strong trapping potentials, while greater altitudes predict smoother trapping potentials. In fact, Brownian motion will ensure that a real particle will explore a variety of altitudes above the surface.
   Note: Computational resources and time will vary with numerical system size, numerical method, and computer hardware.
7. Repeat steps 1.2.5 and 1.2.6 for polarization aligned with each of the other two polarization-distinct C-shape orientations, as polarization angle is taken modulo 180°.
8. For each simulation in the three batches, calculate the net force on the particle by integrating the flux of the Maxwell-Minkowski Stress Tensor through a surface which completely encloses the particle but does not cross any material interfaces.

Copyright © 2015 Journal of Visualized Experiments

9. For each polarization, calculate the work done against optical forces by performing a path integral of the negative net optical force over the path that the particle follows in each batch, as shown in **Figure 3**.

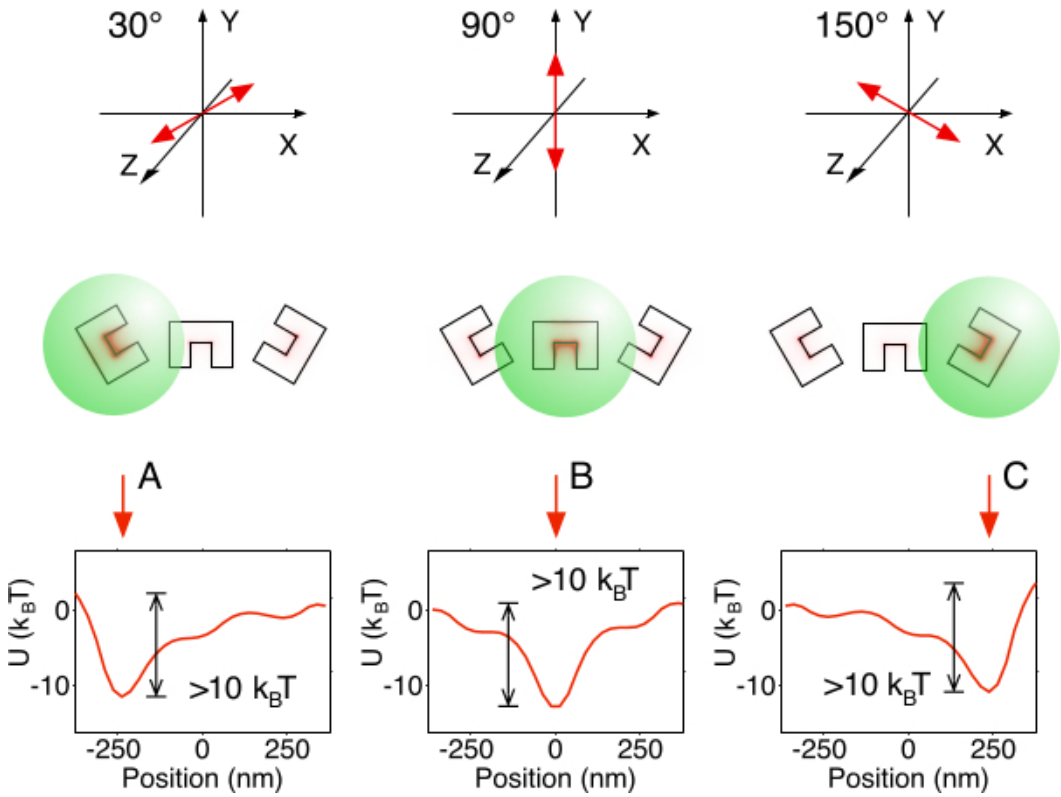

Figure 3. Trapping Verification. Stable trapping can be demonstrated by plotting the optical potential of activation states. A single period of just three CSEs is analyzed for simplicity. Indeed, overall trap depth is sufficient (> 10 k_BT) for stable trapping at the activated engraving for each state A, B, and C. Please click here to view a larger version of this figure.

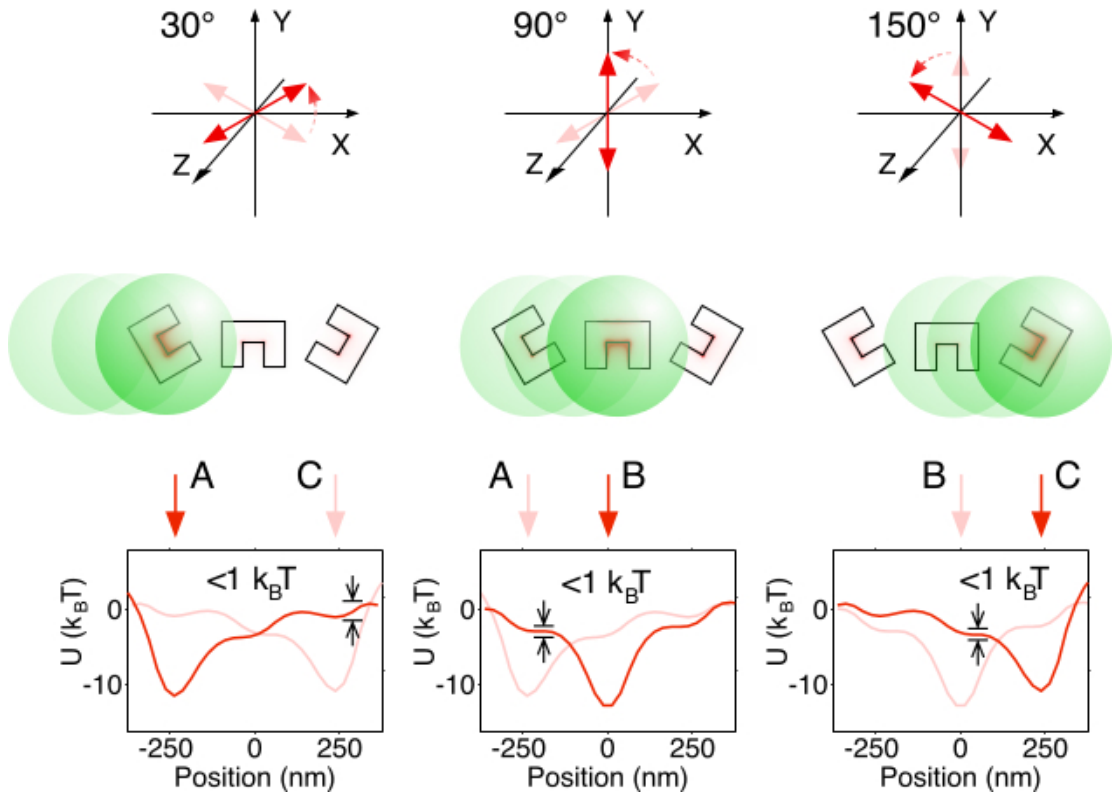

Figure 4. Handoff Verification. Handoff can be demonstrated by plotting the optical potential of old (light red) and new (bright red) activation states in sequence. A single period of just three CSEs is analyzed for simplicity. During handoff from A to B and B to C, the potential barrier in the direction of desired motion between those two positions is both small (1 k_BT) and smaller than that in the opposite direction, indicating that controlled handoff is likely. Handoff from C to A is most difficult because the inter-trap barrier remains sizable at all polarizations. Please click here to view a larger version of this figure.

10. Verify for each polarization A, B, and C that there is an energy barrier of at least 10 k_BT in height on either side of the potential minimum in each period of three Cs. Refer to **Figure 3** for a visual identification of the potential minima and barriers.
    Note: This step determines whether the particle will be stably trapped on the proposed conveyor belt without skipping back and forth. Due to the linearity of electromagnetic waves and the use of linear material models, the energy barrier is proportional to the exciting plane wave intensity.
11. Verify that the energy barriers between adjacent A traps and B traps dip below 1 k_BT when the polarization is continuously rotated from A to B during particle handoff. Repeat for polarization rotation from B to C, and from C to A. Refer to **Figure 4** for a visual identification of these handoff transition potential minima and barriers.
    Note: This step determines if the particle will reliably transfer from a trap A to a trap B during polarization rotation. A particle will easily overcome a barrier of height 1 k_BT to move to a deeper potential well.
12. If there is any insufficient energy barrier in step 1.2.10 or any energy barrier which is too strong in step 1.2.11, adjust the design. In general, to raise energy barriers, increase the space dividing C-shaped engravings. To lower energy barriers, bring the engravings closer together. Avoid bringing them closer together than two skin depths (40 nm), as engravings which are too close together may disrupt one another's resonance currents, which lowers overall trapping effectiveness. Repeat step 1.2 to re-verify the optical potential.

2. Fabricate the CSE Array

Note: The process diagram is shown in **Figure 5**. This process is inspired by the work in ref. 25 and 26.

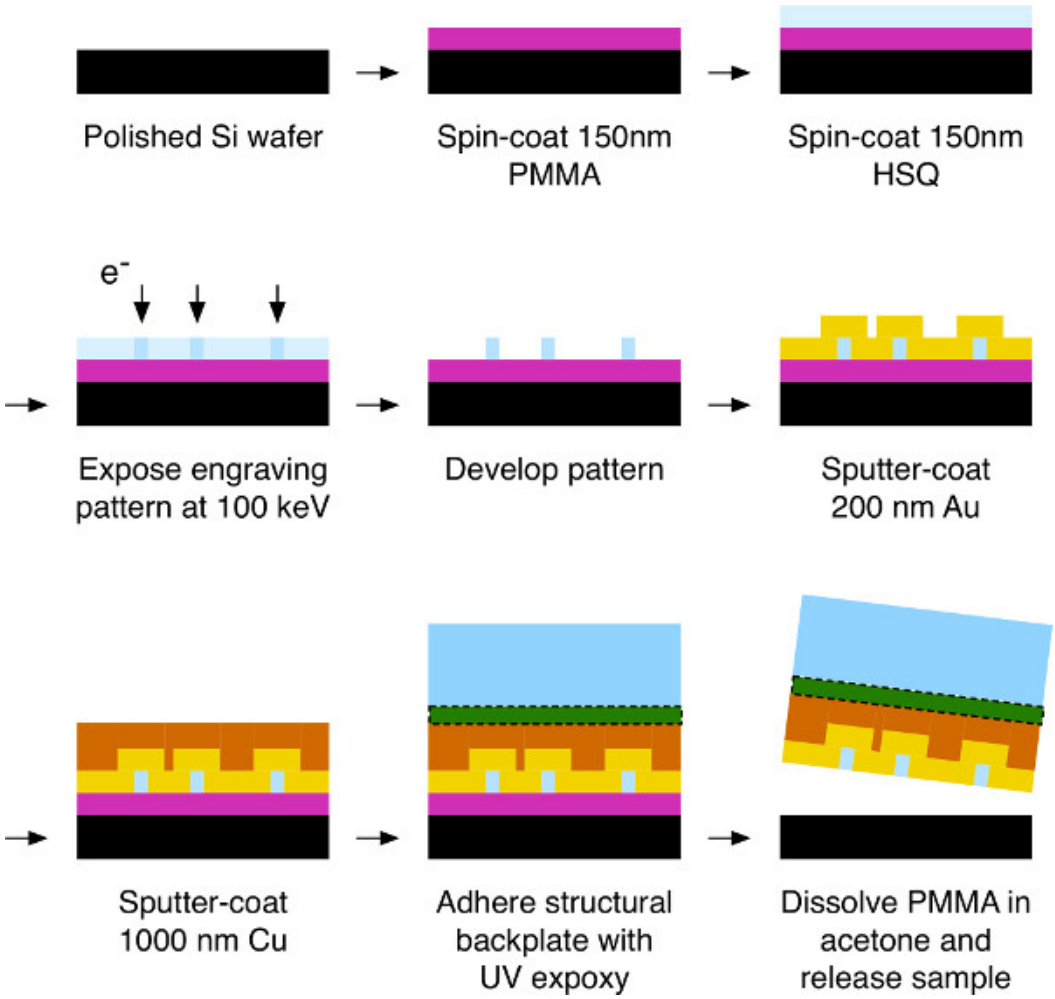

Figure 5. CSE Process. Process flow diagram of the dual-layer template-stripping process. E-beam lithography with 100 keV energy is used to expose the conveyor pattern on the HSQ resist. The thin PMMA layer underneath the HSQ is intended to facilitate the final strip-off (release) of the device from the Si substrate. Please click here to view a larger version of this figure.

1. Acquire a clean, polished silicon wafer and bring it to a clean room equipped for silicon lithography processes.

2. Clean the silicon wafer to remove organic contamination and oxides on the surface.
    1. Immerse the wafer in a 9:1 H_2SO_4:H_2O_2 solution at 100 °C for 10 min. A bath of at least 1 L ensures robust cleaning, though less chemical may permit safer and easier wafer processing as facilities require.
    2. Dip the wafer in a 50:1 HF solution for 30 sec. A bath of at least 1 L ensures robust cleaning, though less chemical may permit safer and easier wafer processing as facilities require.
    3. Thoroughly rinse the wafer with DI water and spin-dry it.

3. Spin coat 50 nm PMMA (thickness is not critical).
    1. Singe bake the wafer at 150 °C for 30 min.
    2. Spin coat a polished, clean silicon wafer with 2% 950k poly-methyl-methacrylate (PMMA) at 5,000 rpm for 40 sec. Apply the PMMA with a pipette, landing 20-25 drops of resist on the center of the wafer before beginning the spin.
    3. Post bake PMMA resist on hotplate at 200 °C for 2 min.

4. Spin coat 150 nm HSQ (same day as following step).
    1. Spin on HSQ negative tone resist at 900 rpm for 1 min. Apply the HSQ with a plastic pipette, again landing 20-25 drops of resist on the center of the wafer before beginning the spin.
    2. Post bake HSQ resist on hotplate at 80 °C for 2 min.

5. Expose and develop the pattern using electron beam lithography techniques (same day as previous step). The process follows from the PMMA/HSQ dual-layer demonstration in ref. 27.
    1. Translate the silhouette design to GDSII format for electron beam patterning in a dose array. Include alignment marks and annotations which are at least 5 µm in size in order to identify the nanostructures under an optical microscope. The dose array should range from 800-4,000 µC/cm^2.
    2. Use an electron beam lithography exposure tool to expose the array at 100 kV accelerating voltage and an aperture of 60 µm, which produces a current of 500 pA. Electron beam exposure is also possible under lower accelerating voltages provided the beam current, dose, and proximity pattern correction are adjusted accordingly.
    3. Develop the exposed HSQ by submerging the wafer in a 2.2% tetramethylammonium hydroxide (TMAH) developer solution for 90 sec. Gently agitate the solution by jostling the developer dish every 10 sec. After the development time has passed, immediately stop the development by flushing the surface with water for 60 sec.

6. Coat a layer of gold 200 nm in thickness, followed by a layer of copper 1,000 nm in thickness, by magnetron sputtering. Make sure to use a sputtering tool whose gold sputtering rate has been calibrated so that the target thickness is achieved within 20%. Sputtering rates will vary among tools. Overshoot in gold thickness is acceptable, as is overshoot in copper.
7. Glue a 1 cm x 1 cm quartz back plate onto patterned substrate with UV-curable epoxy.
    1. Spread a single drop of UV-curable epoxy onto the copper side of the sample in a 1 cm x 1 cm square covering the patterned device area.
    2. Apply a quartz/glass back plate to the copper surface, making sure that it completely covers the patterned device area.
    3. Put on UV safety goggles.
    4. Rest the back plate and wafer on a level surface, and illuminate the epoxy from above with a UV flood lamp for approximately 30 min.
    5. Turn off the UV flood lamp and remove the cured sample.

8. Release the device from the silicon substrate in an acetone bath.
    1. Using a sharp knife, score a smooth, closed path around the quartz back plate, making sure that the cut is deep enough to penetrate all the way through the two metal layers and the PMMA layer above the silicon wafer.
    2. Submerge the substrate in an acetone bath for 6-8 hr.
    3. If after 8 hr the device sample has not yet been released from the silicon wafer naturally, carefully pry the device (including the quartz back plate and both metal layers) away from the silicon wafer using a thin wedge or knife.
    4. Rinse the resulting sample with acetone for about 1 min and dry it with N_2 or clean air.
    5. If there are rough edges of metal or glue remaining around the back plate, carefully trim them away with a razor or lab shears. This will improve the fluid dynamics during a trapping experiment by ensuring uniform evaporation around the chip edges.
    6. Store the sample in a clean, dust-proof container for transport to the optical lab.

3. Prepare the Specimen Sample

1. Prepare a fluorescent polystyrene bead solution.
    1. Dilute a fluorescent polystyrene bead solution from the manufacturer's concentration to 1x10^9/ml– 1x10^{10}/ml by adding the appropriate volume to 1 ml of water.
    2. Add 0.05 ml of surfactant (octyl phenol ethoxylate) to the specimen sample. The surfactant reduces the tendency of the colloidal beads to stick to any surfaces, and it also slightly increases the viscosity of the host fluid.

4. Calibrate the Focus of the Optical Columns

Note: A schematic of the apparatus can be referenced in **Figure 8**.

1. Calibrate the focus of the specimen imaging camera.
    1. Acquire a spare, patterned, and flat reflective surface for testing and calibration. A dummy sample with alignment marks works well.
    2. Turn on the microscope mercury lamp and wait until the light level has stabilized, then open the lamp shutter.

3. Place the patterned test surface into the microscope field of view and move its edge into the field of view center. Adjust light attenuators to make sure that the light is not too bright to observe through the eyepiece, then look through the eyepiece and bring the edge into focus.
4. Move the microscope stage so that a pattern is now in the center of the field of view, and adjust the focus knob to maximize the sharpness of the pattern.
5. Turn on the specimen imaging camera and adjust the brightness and contrast to the microscope illumination level.
6. Adjust the specimen camera focus until the pattern is also in focus for the camera. The pattern should be in focus in both the camera's view and in the eyepiece without having to make any focal adjustments when switching between the two.

2. Calibrate the beam imaging column to ensure that the laser beam imaging camera focuses on the substrate.
Note: It is assumed that the near-IR laser has already been roughly collimated and aligned with the microscope imaging columns. An IR sensor card is a useful tool to perform this alignment. It is recommended to build the whole system on a pre-aligned support such as a cage system so that all of the optics can be centered on the same axis automatically. Dichroic mirrors inserted to separate beam and imaging wavelengths are standard, but for safety should not leak more than 1% of the laser wavelength.
    1. Ensure that each researcher in the room puts on laser safety goggles with an extinction of at least 10^7 at the wavelength of laser operation (1,064 nm) and ensure that the laser beam shutter is closed.
    2. Turn on the laser power supply and cooling system, but leave the beam shuttered. Warm up the laser gain medium.
    3. Once the goggles are in place and the shutter is confirmed closed, turn on the laser. Place a beam block in front of the laser and open the shutter to measure the output of the laser beam and verify, using a power meter, that the laser power output has stabilized. Keep the beam block in place.
    4. To protect the specimen imaging camera from damaging levels of laser light, make sure beam attenuators are in place in front of the specimen imaging camera, as well as a dichroic mirror to direct the remaining beam energy to a separate beam imaging camera. Also, modulate the power of the laser using attenuators or a polarizing beam splitter so that only a moderate amount of power (10 mW) passes through to the apparatus.
    5. Remove the beam block and allow the beam to travel through the apparatus and fall onto the beam imaging camera detector.
    6. Turn on the beam imaging camera and adjust the brightness and contrast to the laser light level.
    7. Defocus the laser beam so that a wide area of the patterned reflector is illuminated by laser light.
    8. Adjust the focus of the beam imaging camera until the features of the pattern are in focus simultaneously with the white light image of the specimen imaging camera, and translate the camera so that its field of view is centered on the field of view of the specimen imaging camera. The effective focal offset between the white light image and the beam image counteracts the focal length discrepancy of the optics between the laser and visible wavelengths.

3. Bring the laser into focus with the beam imaging camera.
    1. Using the calibrated focus in the beam imaging camera, adjust the laser beam focus until it focuses to a tight spot, and adjust the beam's focus position so that it falls in the center of the field of view. Using annotation software or another method of choice, mark the location of the beam in the specimen camera's field of view.
    2. Close the laser beam shutter.

5. Trap and Manipulate Specimen with Optical Energy

Note: A schematic of the apparatus can be referenced in **Figure 8**.

1. Image the fluorescent polystyrene beads.
    1. Replace the dummy sample and cover slip with a clean coverslip in the sample holder of the microscope.
    2. Place a tip on the discharge end of the micro-pipette and extract 2-4 µl of diluted fluorescent particle solution with the pipette.
    3. Slowly discharge the solution onto the coverslip. If there are bubbles, remove them by gently blowing clean air onto the drop of solution.
    4. Carefully place the device on top of the solution blob with gold surface facing down. The solution should spread across the entire area under the device.
    5. Move the microscope stage so that an edge of the resonator array chip is near the center of the field of view. Establish focus on the edge of the chip.
    6. Translate the microscope stage so that the resonator pattern is near the center of the field of view. Focus on the nanostructures by bringing dark alignment marks into focus, and note that the resonators themselves appear as dark spots in the bright reflector background.
    7. Insert a narrow band-pass filter in front of the mercury lamp which blocks all colors other than that corresponding to the fluorescent beads' absorption peak.
    8. Insert a narrow band-pass filter in front of the specimen imaging camera which blocks all colors other than that corresponding to the fluorescent beads' emission peak.
    9. Bring the fluorescent image of the beads into focus, noting their collective average drift velocity against their individually random Brownian motion. Wait until the beads' average drift velocity slows to less than 10 µm/sec.
    Note: Due to evaporation at the edges of the chip, and due to dynamic settling forces of the fluid underneath the chip's weight, there may be visibly apparent currents (tens of µm/s or more) in the specimen fluid. If the evaporation is not too asymmetric along the edge of the chip, these currents will eventually diminish to acceptable levels to perform an experiment.

2. Use the focused laser beam to trap a polystyrene bead.
    1. Ensure that all researchers put on appropriate laser safety goggles, and then turn on the laser while keeping the laser beam shutter closed. Make sure that the laser output is less than 10 mW. Ensure that the laser power has stabilized by testing the beam output with a beam block in place which prevents laser radiation from entering the microscope.

2. Once the laser power has stabilized, remove the beam block and note the laser spot in the beam image. If the spot is out of focus, adjust the laser focus until minimal spot focus is achieved.
3. While ensuring that sufficient attenuators are placed in front of the beam image to prevent beam detector saturation, gradually increase laser output power until a drifting bead can be captured stably at the beam focus. Scanning the microscope stage can assist in trapping a bead which is off-center.
4. Verify that the trapped bead is located at or near the mark made earlier to track the laser focus position in the specimen image. If there is a difference between the bead position and the laser focus mark, correct the laser focus mark to match the new bead position.
5. Now, adjust the beam contractor built in to the beam path until the beam spot is expanded to 9 µm in diameter FWHM when it is fully in focus. Measure this as a straight intensity cross section through the center of the beam spot in the beam image.
6. If the original trapped bead was lost during this adjustment, use the translation stage to search for and trap another bead.
    1. If widening the beam spot has de-stabilized the optical trap (due to a decreased intensity gradient), increase the beam power as necessary to achieve stable optical trapping. If increasing the focal spot size has moved the center of the beam away from its original position, re-mark the average position of the trapped bead in the specimen image as the beam center.

3. Establish near-field trapping and manipulate a polystyrene bead on a C-shaped engraving array.
    1. Turn on the background illumination lamp and increase its power until the substrate pattern can be seen in the background behind the images of fluorescent beads.
    2. With a bead trapped by the loosely-focused beam, use the microscope stage to move the substrate pattern so that the end of an array of resonators can be seen directly behind the trapped bead. If the bead's random Brownian motion becomes significantly reduced, this means the bead is trapped by the near field of an excited resonator.
    Note: If the bead has not yet been trapped by the optical near field, adjust the position of the plasmonic resonator array underneath the bead. This adjustment might bring the bead into closer contact with a resonator which is better aligned with the current polarization of the laser light. If this process does not induce near-field trapping, the beam focus may be slightly above the substrate plane. In this case, adjust the laser focus slightly so that the focal spot approaches the surface of the substrate.
    3. If after small stage and laser focus adjustments the bead has still not yet been trapped by the optical near field, find another array on the substrate and repeat the near-field trapping process, starting with step 5.3.2.
    Note: Fabrication defects cause both systematic and random variations in resonator performance. Non-functioning resonator arrays are common until the fabrication results have been fully characterized and are repeatable.
    4. Once near-field trapping has been established, move the microscope translation stage so that the center of the laser spot resides more near to the center of the conveyor. This action will tend to pull the bead along with the center of the focused laser, so only small adjustments can be made in this way. If a bead becomes dislodged, reduce the motion. This is the amount of beam displacement tolerable by the near-field traps.
    5. After displacing the beam slightly in the previous step, rotate a half-wave plate placed in the laser beam path to rotate the angle of linear polarization. This activates resonators in a sequence down the array and induces controlled, linear motion in the fluorescent bead. A motorized rotary stage can help produce more steady rotation in the half-wave plate and therefore more steady bead motion.
    6. To track the progress of the bead and capture data on its position, turn off the background illumination lamp and use a video capture utility to capture frames of the bead motion. Post-processing of the particle motion can be achieved using the provided MATLAB script.

Representative Results

Figure 7 is a picture of the final device. At the center of the 1 cm x 1 cm gold surface is the matrix of CSE and conveyor patterns, which can be barely seen from an angled view. **Figure 6** is a scanning electron microscopy image of an example CSE pattern on the final device.

The particle motion of a 390 nm polystyrene bead traveling across a nano-optical conveyor belt 5 µm in length is shown in **Figure 9**. The curve shows the particle's position as a function of laser polarization angle. As mentioned in the protocol, there may be cases where transport does not succeed or near-field trapping does not initiate. The best course of action is to try a different pattern, which may be in better condition.

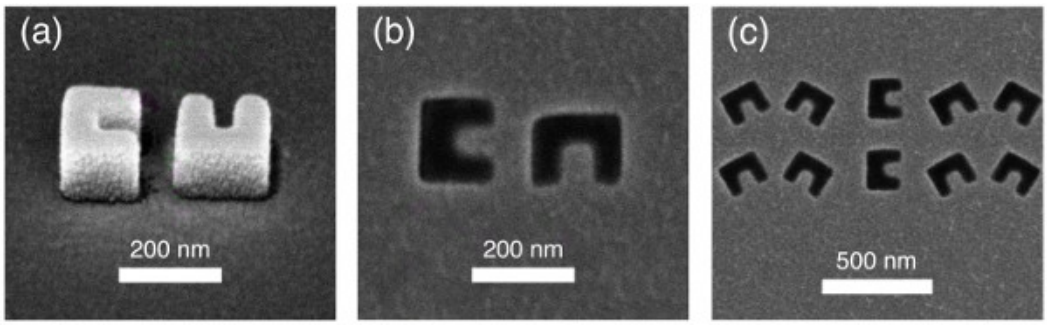

Figure 6. SEM image of CSE Array. Scanning electron microscope (SEM) images of the CSE patterns. (a) shows the picture of HSQ mesas after the resist development. The sample is sputtered with 5 nm gold as a conducting layer for SEM inspection. (b)-(c) show final patterns after the sample is released from the silicon substrate. Please click here to view a larger version of this figure.

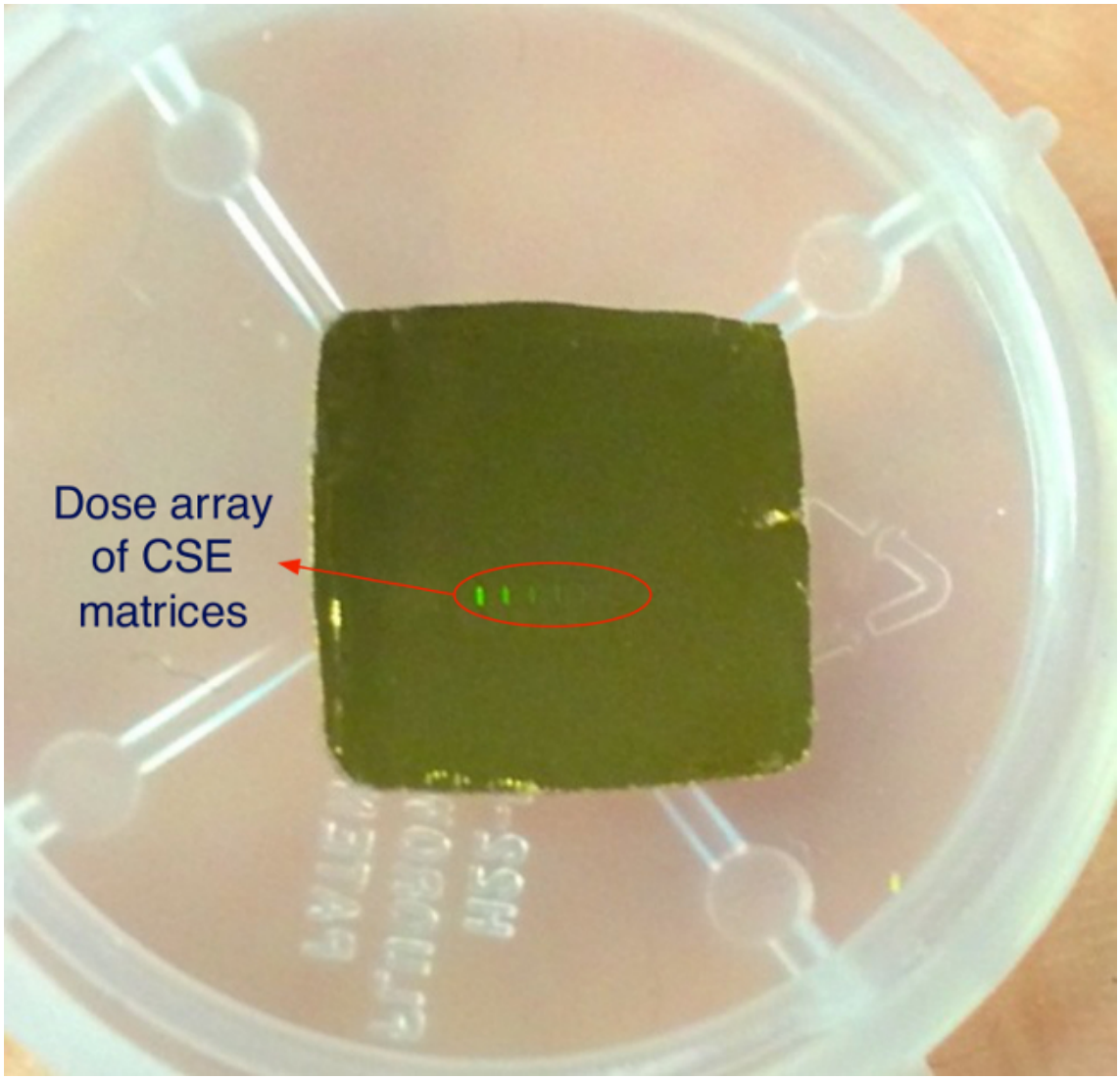

Figure 7. CSE Array Chip. Picture of the final device, roughly 10 mm x 10 mm in dimension. The picture shows the front gold surface of the device. Diffraction from grating ID markings is visible as multi-color squares near the center of the chip. Please click here to view a larger version of this figure.

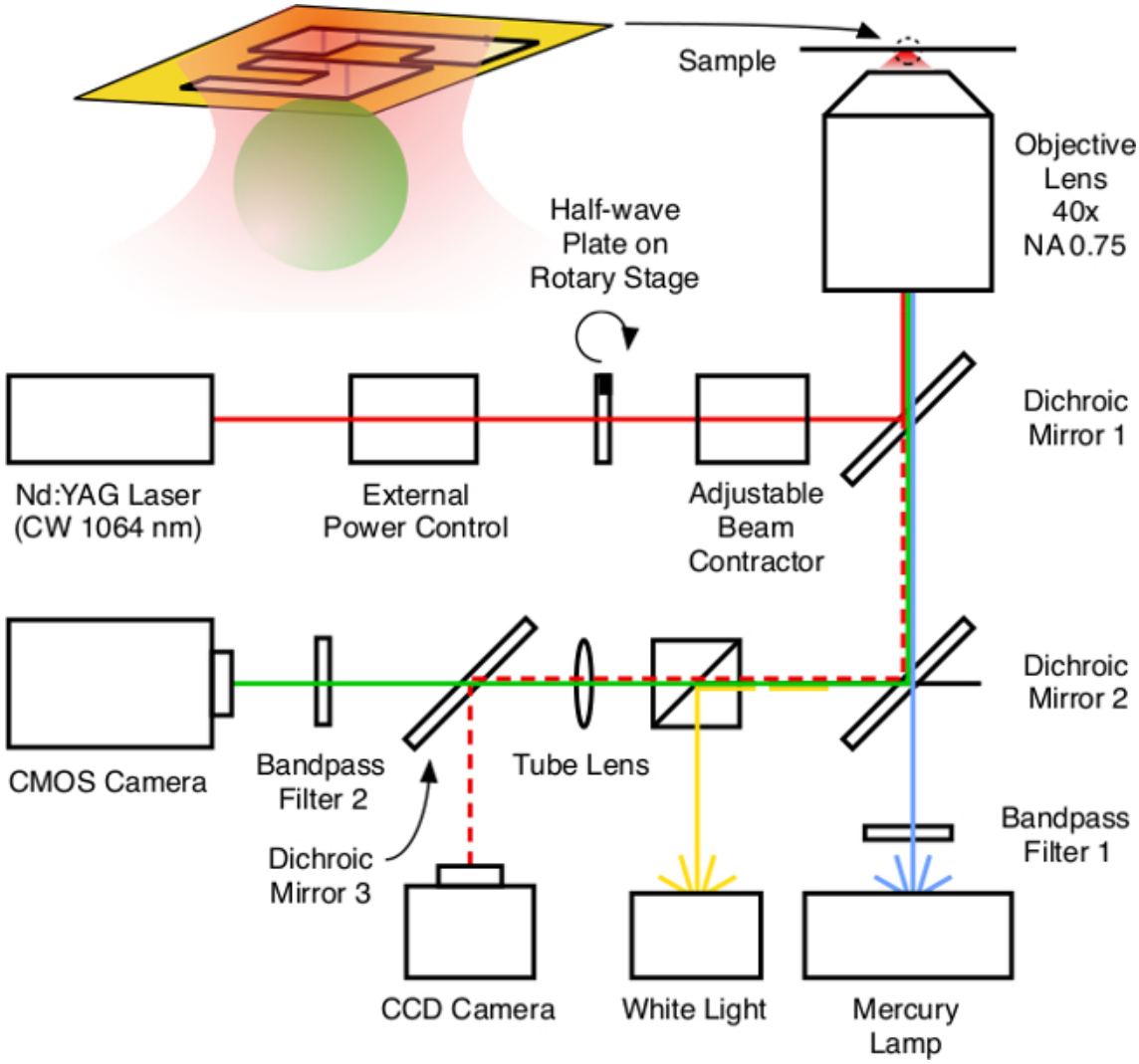

Figure 8. Experimental apparatus. Schematic of the experimental apparatus. Both trapping and imaging are performed in reflection mode. The different light paths are distinguished using different colors. The red, green, dashed red, blue and yellow lines represent the light paths of optical trapping (conveyor driving), fluorescent imaging, laser imaging, fluorescent excitation and bright field illumination respectively. Please click here to view a larger version of this figure.

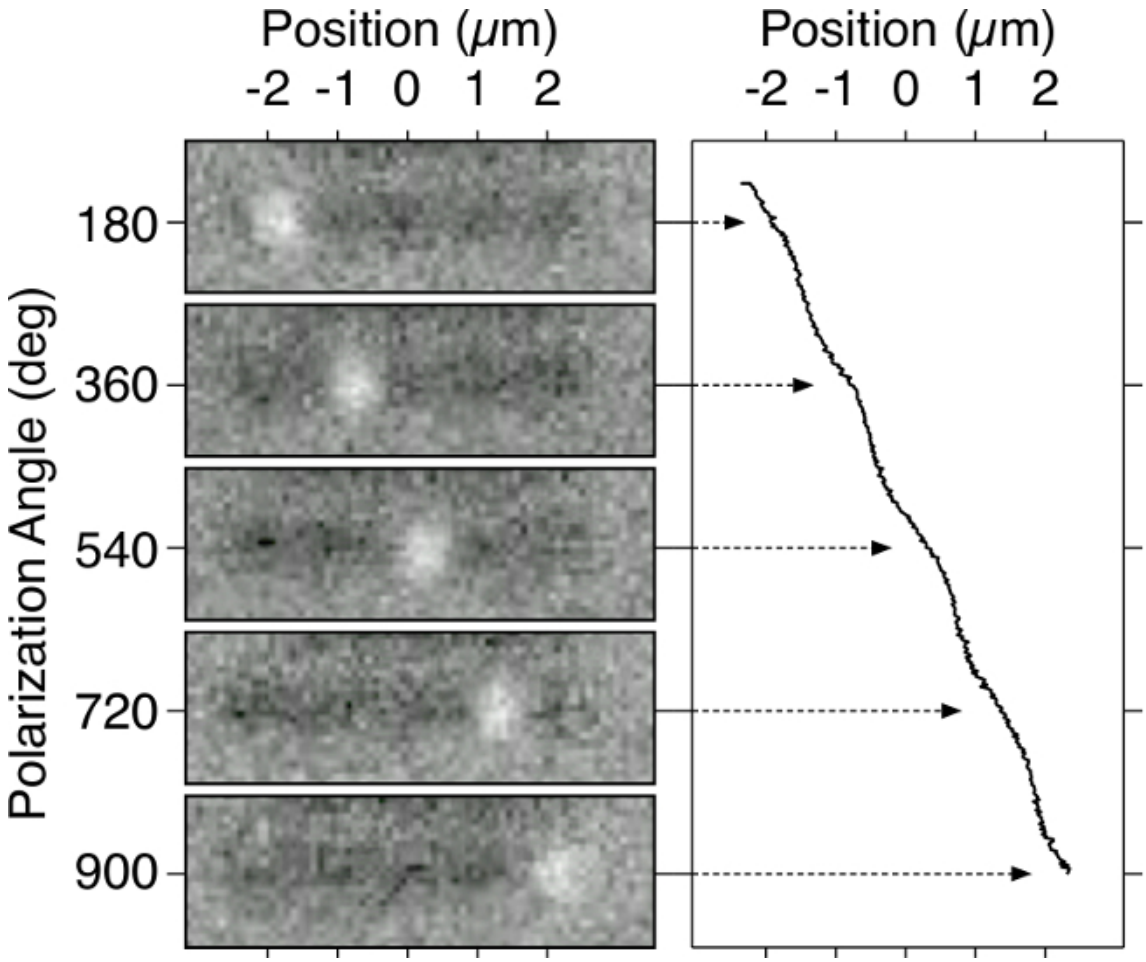

Figure 9. Bead Trajectory Over Double-Rail Conveyor. Position vs. polarization angle for a 390 nm bead moving on a 4.5 μm long double-rail conveyor belt. Images on the left show snapshots of the sphere after each conveyor period. The curve on the right traces the calculated position of the bead centers. Please click here to view a larger version of this figure.

Discussion

The NOCB combines the strong trapping forces and small trap size of plasmonic approaches with the capability to transport particles, long available only for conventional focused-beam techniques. Unique to the NOCB, the trapping and transport properties of the system are a result of surface patterning and not of shaping the illumination beam. Provided the illumination is bright enough and its polarization or wavelength can be modulated, particles can be held or moved in complicated protocols on the surface. We have demonstrated through simulation that an NOCB can also rapidly sort particles based on their mobility[23]. Near-field traps can serve as small reaction volumes for single-molecule chemistry, and the inherent parallelizability of the NOCB means it can be used to set up, perform and tear down as many simultaneous experiments as can be packed onto a chip and illuminated at once.

To get the NOCB to work, the near-field optical forces that hold and hand off nanoparticles must overcome the competing forces of viscous drag, conventional optical trapping (the force of the illumination beam), thermophoresis, and contact forces with other particles and the substrate itself. The near-field optical force should be as strong as possible for a given illumination power; this requires careful nanostructure design and fabrication, but in practice we need to produce a range of structures with different characteristic sizes to select the one that works the best for the given illumination wavelength. The viscous drag and thermophoresis must be suppressed as well: while they may not be able to pull particles out of near-field optical traps, they can certainly make it difficult to get a particle onto the NOCB array in the first place.

When the sample is first placed under the microscope, particles will distribute evenly throughout the volume and very rarely come near to the CSE array. (Calculations indicate that a particle must move within a few tens of nanometers of surface contact to be trapped.) When the illumination is initially turned on, the CSE array will immediately heat up and create a thermal gradient in the water that repels particles over a distance of several hundred nanometers. This barrier is overcome by trapping a particle at a distance with the focused illumination beam, and manually dragging the particle through the thermal barrier into the trapping field of the CSE. However even this method will fail if the thermal gradient is too high. In our experience, the inclusion of the copper heat sink layer was crucial for drawing the heat away from the water and weakening the thermal forces. The copper heat sink also makes it less likely that the water will boil under normal illumination intensity.

The optical gradient force on a very small particle scales as the cube of the particle diameter. This makes it much harder to trap a 100 nm bead than a 200 nm bead, since the power must be increased eight times—increasing the substrate heating by the same amount. As a practical

Copyright © 2015 Journal of Visualized Experiments

matter we recommend trapping larger beads first (400 nm or 500 nm diameter), optimizing the trap strength and minimizing competing forces, and then attempting trapping and transport of smaller particles.

Once the sample has been prepared, experiments can be performed as long as the particles are freely floating in water. Water exits the sample by evaporation along the edges. In our lab this puts a roughly 20 min time limit on experiments. Evaporation can also result in a competing viscous drag force as water is drawn to the edges of the sample. If the sample has rough features such as bent-up metal edges or spikes that prevent it from lying flat on the glass slide, the greater exposed surface area of the water will speed evaporation. If one side is higher than the other, the evaporation will be biased towards the side with the larger sample-slide gap and the fluid will move rapidly over the nanostructures, making it harder to see, capture and hold particles.

A single NOCB can transport particles across the width of the illumination beam but no further. As the beam intensity drops off, the restoring force from the focused beam grows stronger and the NOCB handoff force grows weaker, until polarization rotation is more likely to release the particle than move it forward. For extension to longer conveyors or more parallel conveyors, the illumination area must be increased. A powerful, defocused laser diode could power a much larger area than the laser used in these experiments. Alternatively the illumination area can be increased by rapidly scanning the beam using an acousto-optic deflector.

Disclosures

The authors have nothing to disclose.

Acknowledgements

The authors would like to thank Professor Yuzuru Takashima at the University of Arizona for discussions on optical imaging, Mr. Karl Urbanek for assistance with high power lasers, and Max Yuen for discussions of Brownian motion. The authors send further thanks to Professor Kenneth Crozier at Harvard University for helpful discussions on optical trapping experiments. Funding was provided in part by the United States National Science Foundation (award number 1028372).

References

1. Ashkin, A., Dziedzic, J. M. Optical Trapping and Manipulation Of Viruses and Bacteria. *Science.* **235**, (4795), 1517-1520 (1987).
2. Svoboda, K., Block, S. M. Biological Applications of Optical Forces. *Annu. Rev. Biophys. Biomol. Struct.* **23**, (1), 247-285 (1994).
3. Neuman, K., Block, S. Optical Trapping. *Rev. Sci. Instrum.* **75**, (9), 2787-2809 (2004).
4. Fazal, F. M., Block, S. M. Optical Tweezers Study Life Under Tension. *Nat. Photonics.* **5**, (6), 318-321 (2011).
5. Bockelmann, U., Thomen, P., Essevaz-Roulet, B., Viasnoff, V., Heslot, F. Unzipping DNA with Optical Tweezers: High Sequence Sensitivity and Force Flips. *Biophys. J.* **82**, (3), 1537-1553 (2002).
6. Pang, Y., Gordon, R. Optical Trapping of Single Protein. *Nano Lett.* **12**, (1), 402-406 (2012).
7. Dholakia, K., Čizmář, T. Shaping the Future of Manipulation. *Nat. Photonics.* **5**, (6), 335-342 (2011).
8. Grier, D. G., Roichman, R. Holographic Optical Trapping. *Appl. Opt.* **45**, (5), 880-887 (2006).
9. Korda, P. T., Taylor, M. B., Grier, D. G. Kinetically Locked-in Colloidal Transport in an Array of Optical Tweezers. *Phys. Rev. Lett.* **89**, (12), 128301 (2002).
10. Pelton, M., Ladavac, K., Grier, D. G. Transport and Fractionation in Periodic Potential-energy Landscapes. *Phys. Rev. E.* **70**, (3), 031108 (2004).
11. Eriksson, E., *et al.* A Microfluidic System in Combination with Optical Tweezers for Analyzing Rapid and Reversible Cytological Alterations in Single Cells upon Environmental Changes. *Lab Chip.* **7**, (1), 71-76 (2007).
12. Applegate, R. W., Squier, J., Vestad, T., Oakey, J., Marr, D. W. M. *Optical Trapping, Manipulation, and Sorting of Cells and Colloids in Microfluidic Systems with Diode Laser.* **12**, (19), 4390-4398 (2004).
13. MacDonald, G. C., Spalding, G. C., Dholakia, K. Microfluidic Sorting in an Optical Lattice. *Nature.* **426**, (6965), 421-424 (2003).
14. Neale, S. L., MacDonald, M. P., Dholakia, K., Krauss, T. F. All-optical Control of Microfluidic Components using Form. *Nat. Mater.* **4**, (7), 530-533 (2005).
15. Juan, M. L., Righini, M., Quidant, R. Plasmon Nano-optical Tweezers. . *Nat. Photonics.* **5**, (6), 349-356 (2011).
16. Kwak, E. S., *et al.* Optical Trapping with Integrated Near-Field Apertures. *J. Phys. Chem. B.* **108**, (36), 13607-13612 (2004).
17. Righini, M., Zelenina, A. S., Girard, C., Quidant, R. Parallel and Selective Trapping in a Patterned Plasmonic Landscape. *Nat. Phys.* **3**, (7), 477-480 (2007).
18. Zhang, W., Huang, L., Santschi, C., Martin, O. J. F. Trapping and Sensing 10 nm Metal Nanoparticles using Plasmonic Dipole Antennas. *Nano Lett.* **10**, (3), 1006-1011 (2010).
19. Wang, K., Schonbrun, E., Steinvurzel, P., Crozier, K. B. Trapping and Rotating Nanoparticles using a Plasmonic Nano-tweezer with an Integrated Heat Sink. *Nat. Commun.* **2**, 469 (2011).
20. Shi, X., Hesselink, L., Thornton, R. Ultrahigh Light Trans- mission through a C-shaped Nanoaperture. *Opt. Lett.* **28**, (15), 1320-1322 (2003).
21. Chen, K., Lee, A., Hung, C., Huang, J., Yang, Y. Transport and Trapping in Two-Dimensional Nanoscale Plasmonic Optical Lattice. *Nano Lett.* **13**, 4118-4122 (2013).
22. Cuche, A., *et al.* Sorting Nanoparticles with Intertwined Plasmonic and Thermo-Hydrodynamical Forces. *Nano Lett.* **13**, 4230-4235 (2013).
23. Hansen, P., Zheng, Y., Ryan, J., Hesselink, L. Nano-Optical Conveyor Belt, Part I: Theory. *Nano Lett.* **14**, 2965-2970 (2014).
24. Zheng, Y., *et al.* Nano-Optical Conveyor Belt, Part II: Demonstration of Handoff Between Near-Field Optical Traps. *Nano Lett.* **14**, 2971-2976 (2014).
25. Vogel, N., Zieleniecki, J., Koper, I. As flat as it gets: Ultrasmooth Surfaces from Template-stripping Procedures. *Nanoscale.* **4**, (13), 3820-3832 (2012).
26. Zhu, X., *et al.* Ultrafine and Smooth Full Metal Nanostructures for Plasmonics. *Adv. Mater.* **22**, (39), 4345-4349 (2010).

Copyright © 2015 Journal of Visualized Experiments

27. Kaleli, B., *et al.* Electron Beam Lithography of HSQ and PMMA Resists and Importance of their Properties to Link the Nano World to the Micro World. *STW.ICT Conf.* 105-108 (2010).

Copyright © 2015 Journal of Visualized Experiments